

Exploring elemental variability in incineration residues for urban mining: A case study from southern Poland

Barbara Bielowicz*, Monika Chuchro

Department of Geology of Mineral Deposits and Mining Geology, Faculty of Geology, Geophysics and Environment Protection, AGH University of Krakow, Al. Mickiewicza 30, 30-059 Kraków, Poland

* corresponding author; e-mail: bbiel@agh.edu.pl

BB  <https://orcid.org/0000-0002-8742-5890>, MC  <https://orcid.org/0000-0002-0381-4697>

Abstract

Urban mining increasingly concentrates on secondary raw materials derived from waste streams, among which municipal solid waste incineration (MSWI) residues are of growing importance. Fly ash, in particular, contains a wide range of trace and critical elements, yet its variability and internal associations remain insufficiently characterised. In the present study, 30 fly ash samples were collected in 2021 on a weekly basis from an MSWI facility in southern Poland. Eighteen elements (Ag, Al, Au, Ba, Co, Cr, Cu, Fe, Li, Mn, Mo, Ni, Pb, Pt, Sb, Sr, V and Zn) were quantified using ICP-MS and ICP-OES, producing a robust dataset suitable for multivariate analysis. Data exploration comprised descriptive statistics, normality assessment with the Shapiro-Wilk test, outlier detection via Rosner's test, correlation analysis using Pearson's and Spearman's coefficients, and hierarchical cluster analysis (HCA). Results show that most elements display moderate concentrations (10–1000 ppm), while Al, Fe, and Zn exceed 1000 ppm, and noble metals remain below 10 ppm. Strong positive correlations were observed between Sr and Li, as well as Fe, Ni, and Mo, while HCA consistently grouped Cr, Fe, Mo, and Ni into a stable cluster across methods. The most accurate dendrogram structure was achieved with average linkage (Euclidean or Manhattan), whereas Pearson-based distances produced sharper cluster boundaries. Importantly, the elemental concentrations determined in fly ash were systematically compared with both the geochemical background of the Earth's crust and typical grades in natural ore deposits. This comparison revealed substantial enrichment in Zn, Pb, Sb, Ag, Au, and Pt relative to crustal averages, while only Zn (and occasionally Cu and Ag) reached concentrations approaching the lower thresholds of economically exploited ore deposits. These findings demonstrate the internal geochemical structure of MSWI fly ash and underscore its significance as a potential source of valuable elements within the framework of urban mining.

Keywords: Fly ash, critical raw materials, exploratory data analysis, municipal solid waste incineration, sustainable circular economy

1. Introduction

Being faced with the systematic depletion of strategic metal and rare earth element resources, coupled with significant environmental impacts from ore extraction, the concept of urban mining is gaining increasing recognition as an innovative strategy for

sustainable development. Municipal Solid Waste Incineration (MSWI) fly ash represents a particularly intriguing, albeit complex component of this strategy, serving both as hazardous waste and a potential source of valuable raw materials. Some researchers have highlighted the dual nature of these materials, posing both environmental risks

and economic opportunities (e.g. Buha et al., 2014; Fabricius et al., 2020; Kanhar et al., 2020).

Growing evidence suggests that the content of metals like zinc, copper and lead in fly ash can rival or even surpass levels found in lower-grade ores, rendering them valuable from a resource management perspective (Schlumberger & Bühler, 2012; Bakalár et al., 2021). In light of increasing environmental awareness and the implementation of circular economy models, MSWI fly ash may play a pivotal role in 'zero-waste' strategies, integrating waste neutralisation with raw material recovery (Assi et al., 2020; Prasittisopin, 2024).

However, due to the complex chemical and physical properties of fly ash, derived from the variability in waste composition, combustion conditions and flue gas cleaning technologies (Buha et al., 2014; Fabricius et al., 2020), it poses significant challenges for research. The ash contains a mixture of calcium and silicon oxides, sodium and chlorine salts, as well as substantial amounts of heavy metals including zinc, lead, cadmium, chromium, copper and arsenic. Moreover, rare earth elements and phosphorus, whose natural availability is limited (Kalmykova & Karlfeldt, 2013; Lane et al., 2020), are also present.

Sequential extraction studies have shown that a significant portion of these metals exists in readily mobilisable forms, enhancing the risk of environmental migration, particularly under variable pH conditions. Metals such as lead and cadmium are especially prone to this (Huang et al., 2007; Haberl & Schuster, 2019), while zinc mobility increases under alkaline conditions (Yakubu et al., 2018). The physical properties of fly ash, such as density, particle size distribution and the presence of nanometric fractions, are crucial for efficient recovery and potential secondary applications in construction materials (Buha et al., 2014).

Notably, similarities can be drawn with coal combustion ashes, which have been extensively analysed for their impact on health and environment. Although MSWI fly ash differs in composition, containing higher levels of chlorine salts and heavy metals, similar toxicity and mobility concerns necessitate specific stabilisation strategies (Fuoco et al., 2005; Ivan Diaz-Loya et al., 2012; Zierold & Odoh, 2020). Therefore, the dualistic nature of fly ash, being both a hazard and a resource, is a fundamental aspect of evaluating its role in urban mining concepts (Bakalár et al., 2021; Funari et al., 2023).

Furthermore, the necessity for appropriate management of this waste stems from the fact that MSWI fly ash also contains organic and inorganic pollutants, thus posing significant environmen-

tal risks (Kanhar et al., 2020). In mitigating these negative impacts, both stabilisation and solidification processes (Yakubu et al., 2018; Wang et al., 2023) and innovative recovery techniques such as bioleaching or thermal separation are crucial (Lane et al., 2020). Research on the physicochemical properties of fly ash indicates that it is a highly heterogeneous material, with composition dependent on waste types and combustion conditions (Lima et al., 2008). This underscores the importance of studies regarding both environmental safety and valuable element recovery contexts (Wong et al., 2020; Zierold & Odoh, 2020). Therefore, special attention is given to processes for neutralising and reusing fly ash in construction, land remediation and agriculture, although many proposed solutions require long-term stability and efficacy assessments (Joseph et al., 2018; Rusănescu & Rusănescu, 2023).

The economic viability and environmental benefits of urban mining are substantial, transforming waste into a valuable resource. Contemporary approaches to municipal waste management focus not only on volume reduction, but also on recovering valuable raw materials, aligning with circular economy principles (Kravtsova & Volkov, 2015). Ashes from municipal solid waste incineration, often viewed as problematic by-products, are increasingly recognised as potential secondary sources of critical raw materials. The present study examines the chemical composition of MSWI fly ash, focusing on identifying and analysing concentrations of elements with potential economic and strategic significance (İşildar et al., 2018). The analysis aims to identify relationships between elements and assess their co-occurrence, potentially indicating synergies in recovery processes. A detailed understanding of the chemical and mineralogical characteristics of fly ash is key to designing efficient extraction processes while minimising the risk of mobilising unwanted trace elements (Ilyushechkin et al., 2020).

Additionally, the analysis seeks to explore the feasibility of applying innovative technological solutions, such as hydrometallurgical methods, for selective metal recovery from these complex waste matrices (Sobianowska-Turek, 2018). The findings of this research will contribute to the development of urban mining strategies in Poland, highlighting the potential of MSWI fly ash as a valuable resource. Moreover, it supports the transition towards a more circular economy.

In relation to current needs, the objective of the present study is to determine the content of selected elements in MSWI fly ash from a facility located in southern Poland and to compare these values with those found in conventional deposits. This analysis

will assess the potential of the examined fly ash as an alternative raw material source and its significance in developing urban mining strategies in Poland.

2. Material and methods

2.1. Material

The Thermal Waste Treatment Plant located in southern Poland represents a state-of-the-art facility designed for the neutralisation of unsorted municipal solid waste. The plant operates on a reciprocating grate combustion system equipped with a heat recovery boiler and a comprehensive flue gas cleaning line, which includes selective non-catalytic reduction (SNCR) of NO_x , semi-dry absorption using lime slurry and adsorption of heavy metals on activated carbon. The combustion process takes place under high-temperature conditions, with furnace temperatures reaching 850–1000°C. It ensures effective oxidation of organic substances and reduction of gaseous pollutants. In order to comply with environmental protection regulations, flue gas temperature is maintained for at least two seconds above 850°C, thereby guaranteeing the complete destruction of organic compounds, including dioxins and furans. High combustion temperatures, in combination with controlled flue gas residence time in the high-temperature zone and sufficient oxygen supply, promote the complete burnout of waste and minimise the amount of bottom ash residues. At the same time, these parameters exert a significant influence on the formation and chemical composition of slags and ashes, determining the extent of element immobilisation in solid phases and their subsequent environmental mobility or potential for recovery.

The combustion process generates residues in the form of incineration bottom ash (IBA), fly ash (FA) and air pollution control residues (APCr). In the present study, special attention was given to fly ash. In order to characterise the chemical composition of these secondary residues, a systematic sampling campaign of fly ash was carried out in 2021. Samples were collected on a weekly basis over a period of 30 consecutive weeks in accordance with the PN-EN 14899:2006 standard ('Characterization of waste – Sampling of materials – Structure preparation and application of a sampling plan'), which ensured both the representativeness of the collected material and the reliability of the results. During each sampling event, eight primary fly ash samples, each weighing approximately 3.5–4.0 Mg, were collected directly from the end of the conveyor belt,

from the falling stream of waste, using a wheel loader equipped with an automatic weighing system. From these, a composite sample with a total weight of up to approximately 32 Mg was formed and subsequently subjected to a multi-stage reduction process. First, the material was arranged in a rectangular two-layer prism, each layer containing four of the original samples. The prism was divided into two equal parts by excavating it from the shorter side; one half was directed to the next stage of reduction, while the other half was discarded. This procedure yielded two reduced prisms of about 8 Mg each. Material was then taken along the mid-section of these prisms to obtain approximately 300 kg of representative sample, which was further reduced using a sample splitter to produce laboratory samples weighing around 10 kg each.

Prior to chemical analysis, the fly ash was weighed and dried, then crushed using a Terminator Jaw Crusher TM Engineering so that more than 70 per cent of the material passed through a 2-mm-sieve. Approximately 250 g of the crushed fraction was further ground in an LM201 ESSA FLSmidth grinder to obtain a homogeneous material with a particle size below 75 μm . For chemical digestion, a modified aqua regia solution consisting of equal parts of concentrated HCl and HNO_3 with distilled water was used, and digestion was carried out for one hour in a block heater. The digested solutions were then diluted with diluted HCl to the required volume.

All chemical determinations were performed at Bureau Veritas Commodities Canada Ltd. (Vancouver, Canada), an accredited laboratory specialising in geochemical and environmental analyses. The prepared samples were analysed using inductively coupled plasma mass spectrometry (ICP-MS) on an ELAN 9000 spectrometer for trace and ultra-trace elements, and by inductively coupled plasma optical emission spectrometry (ICP-OES) on a Ciros Vision spectrometer after borate flux fusion for the determination of major and minor elements. The use of certified reference materials, analytical blanks and duplicate samples ensured the high quality and reliability of the data obtained, which subsequently provided the basis for the statistical evaluation of the chemical composition and variability of the fly ash examined.

2.2. Data

The analysis was carried out for 18 elements determined in fly ash originating from the combustion of municipal solid waste. Individual samples were

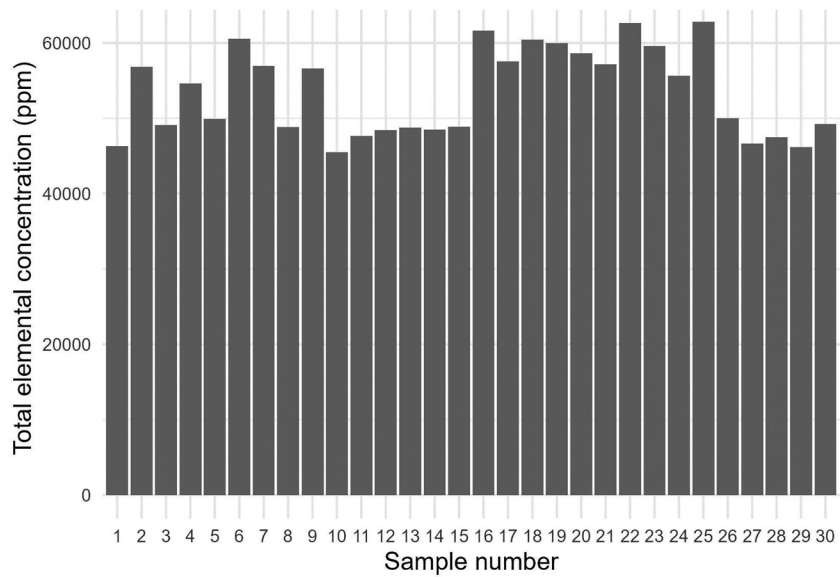


Fig. 1. Cumulative concentrations of selected elements in fly ash examined.

collected on a weekly basis throughout 2021. Sampling, sample preparation and quantitative determination of selected elements were performed in accordance with standardised procedures. For the exploratory data analysis, the following elements were considered: silver (Ag), aluminum (Al), gold (Au), barium (Ba), cobalt (Co), chromium (Cr), copper (Cu), iron (Fe), lithium (Li), manganese (Mn), molybdenum (Mo), nickel (Ni), lead (Pb), platinum (Pt), antimony (Sb), strontium (Sr), vanadium (V) and zinc (Zn). The dataset comprised 30 observations, without missing values or censored results, and all elemental concentrations were expressed in ppm. The cumulative content of elements in the fly ash samples is presented in Figure 1.

2.3. Methods

The exploratory data analysis was conducted at three stages. At the first stage, a descriptive analysis of the dataset was carried out, including basic summary statistics and tests of normality and Rosner test. At the second stage, attention was directed towards assessing the relationships among the studied elements. For this purpose, correlation matrices were constructed using both Pearson's product-moment correlation and Spearman's rank correlation. At the final stage, hierarchical cluster analysis was employed to evaluate the similarity of elements to one another. This sequential approach provided a comprehensive framework for understanding the statistical structure of the dataset.

The Shapiro-Wilk test remains one of the most widely applied statistical procedures for assessing

the conformity of a variable's distribution with the normal distribution. Its key advantage lies in its relatively high statistical power, especially for small to medium sample sizes, compared with other normality tests such as the Kolmogorov-Smirnov or Lilliefors tests. The test statistic is based on comparison of the ordered values of the sample with the corresponding quantiles of the normal distribution. Results are expressed in the form of a p-value, where failure to reject the null hypothesis ($p > 0.05$) indicates that the data are consistent with normality (Shapiro & Wilk, 1965).

Rosner's test, also known as the Generalised Extreme Studentised Deviate (ESD) test, is designed for the detection of multiple outliers in univariate datasets. This method extends the classical Grubbs' test by allowing for the identification of more than one outlier within a sample. The test iteratively removes the most extreme observation(s) and evaluates their statistical significance based on the calculated test statistic. It is particularly useful in environmental, geochemical and industrial applications, where the presence of outliers can considerably affect the interpretation of results (Rosner, 1983).

Pearson's correlation coefficient describes the linear relationship between two continuous variables. Its value ranges from -1 to +1, with coefficients approaching either extreme indicating a strong linear association, while values near 0 suggest the absence of a linear correlation. In contrast, Spearman's rank correlation coefficient (ρ) measures the degree of monotonic association between variables by comparing their ranks and does not require the assumption of normality (Hand et al., 2001). Consequently, it is appropriate for cases where the assumptions of

Pearson's test are not met, or when relationships are monotonic but nonlinear. Employing both correlation approaches enables a more robust assessment of relationships, particularly in datasets combining normally and non-normally distributed variables (Hauke & Kossowski, 2011; Headrick, 2016).

Hierarchical cluster analysis (HCA) is a widely used technique for grouping observations based on their similarity, quantified using distance metrics such as Euclidean, Manhattan or correlation-based measures. The procedure can be implemented in an agglomerative manner (progressively merging single elements into larger clusters) or in a divisive manner (splitting the dataset into progressively smaller groups). The results are typically visualised in the form of dendograms, which facilitate interpretation of the relationships among variables and observations. In the present study, different distance metrics and linkage methods were evaluated to ensure robustness of clustering results (Murtagh & Contreras, 2011; Nielsen, 2016). The most informative and consistent outcomes were obtained for the following combinations: Euclidean + Ward.D2, Euclidean + Complete, Euclidean + Average, Manhattan + Complete, Manhattan + Average, and 1 - Pearson + Complete. These variants were selected for further interpretation and are presented in the

section 'Results', allowing direct comparison of the clustering approaches in terms of their ability to capture geochemical relationships. This method has found broad application in geochemistry, molecular biology and environmental sciences. Two quality measures were employed to evaluate clustering results. The agglomerative coefficient (AC) reflects how strongly the data are structured into clusters during the agglomerative process; higher values (approaching 1) indicate more distinct and coherent clusters (Kara, 2021). In turn, the cophenetic correlation coefficient (CCC) assesses how well the dendrogram preserves the original pairwise distances between objects. Values closer to 1 suggest that the hierarchical tree accurately represents the underlying data structure (Sokal & Rohlf, 1962).

3. Results

3.1. Descriptive statistics

To provide an overview of the chemical variability of fly ash, descriptive statistics were first calculated for all elements analysed. This step enabled the identification of general concentration ranges, as-

Table 1. Descriptive statistics in fly ashes in ppm and earth crust content (¹ Rudnick & Gao, 2003; ² Kabata-Pendias, 2011; ³ Valero & Valero, 2014; ⁴ British Geological Survey, 2025; ⁵ United States Geological Survey, 2021; ⁶ United States Geological Survey, 2024).

Element [ppm]	Min	Median	Mean	Max	Sd	Earth crust content ^{1,2}	Ore deposits ^{3,4,5,6}
Ag	3.20	4.85	4.96	6.87	0.89	0.07	50–300 in Ag–Pb–Zn ores
Al	28,000.00	32,750.00	33,263.33	40,000.00	3563.37	82,000.00	238,000–318,000 Al in bauxite
Au	0.009	0.025	0.031	0.075	0.017	0.0015	5.26 average in gold
Ba	90.30	121.85	130.66	234.20	36.18	630.00	118,000–206,000 Ba in barite ores; up to 559,000 in concentrates
Co	16.00	24.25	24.39	33.10	4.11	17.00	~3000 Co in sediment-hosted Cu–Co ores
Cr	107.90	142.70	146.85	213.80	24.35	92.00	274,000–342,000 Cr in chromite ores
Cu	241.49	350.35	357.79	567.39	69.78	28.00	4000–7000 Cu in porphyry ores
Fe	9900.00	13,300.00	13,640.00	18,600.00	2367.25	50,000.00	250,000–660,000 Fe in iron ores and concentrates
Li	9.70	11.65	12.11	15.70	1.72	20.00	4600–9300 Li in pegmatites; 200–1400 Li in brines
Mn	519.00	686.50	688.33	863.00	88.74	600.00	350,000–440,000 Mn in manganese ores
Mo	7.44	10.07	10.42	17.23	2.03	1.10	500–3000 Mo in porphyry ores
Ni	48.00	65.20	68.75	125.30	17.96	47.00	8000–30,000 Ni in sulfide/lateritic ores
Pb	185.54	329.84	369.10	708.97	132.33	17.00	34,000 Pb average
Pt	0.027	0.036	0.036	0.066	0.008	0.0005	1–5 Pt in PGE reefs
Sb	111.20	143.81	144.05	224.17	20.88	0.20	10,000–100,000 Sb in stibnite ores
Sr	245.70	298.65	301.29	379.30	37.60	320.00	439,000 Sr in celestine ores
V	22.00	26.00	25.80	30.00	2.20	97.00	1100–8400 V in titanomagnetite/uraniferous sandstones
Zn	3154.10	4093.20	4255.17	5711.40	681.91	67.00	5000–10,000 Zn in Zn–Pb ores

essment of distributional properties and detection of potential outliers that could influence further statistical analyses.

The normality of the distributions of elemental concentrations was assessed using the Shapiro-Wilk test ($\alpha = .05$). Seven elements (Au, Ba, Li, Mo, Ni, Pt and Sb) exhibited significant deviations from normality ($p < .05$), while the remaining eleven elements (Ag, Al, Co, Cr, Cu, Fe, Mn, Sr, Pb, V and Zn) did not significantly differ from a normal distribution ($p > .05$). These results provided a basis for applying both parametric and non-parametric statistical tools in subsequent analyses.

The concentrations of individual elements in fly ash were highly variable (Table 1; Fig. 2). Elements with high mean concentrations exceeding 1000 ppm included aluminum, iron and zinc, reflecting their prevalence in municipal waste combustion residues. Elements with moderate mean concentrations (10–1000 ppm) were commoner and encompassed barium, cobalt, chromium, lithium, copper, manganese, molybdenum, nickel, lead, tin, antimony and strontium, of which seven exceeded 100 ppm. Conversely, low or very low mean concentrations were associated with precious metals. In particular, silver, gold and platinum displayed mean concentrations below 10 ppm (Table 1).

Comparison of maximum and minimum values revealed that for eight elements, the maximum did not exceed twice the minimum concentration. In

contrast, for two elements the maximum surpassed three times the minimum, with gold showing the most extreme variation, where the maximum was almost nine times higher than the minimum (Table 1; Fig. 2). When mean and median values were compared, only small differences were observed, typically below 5 per cent. Larger discrepancies were found for gold (18 per cent), lead (11 per cent) and barium (7 per cent). Such small differences indicate relatively symmetric distributions and a limited number of outliers. The presence of outliers was confirmed using Rosner's Generalised ESD test, which is more precise than the conventional 1.5 IQR rule or the 2σ method in cases of skewed distributions. This test identified significant right-sided outliers for copper, molybdenum, nickel, platinum and antimony (Table 1; Fig. 2).

3.2. Correlation analyses

To explore associations among elements, both Pearson's product-moment correlation coefficient and Spearman's rank correlation were applied. The dual approach was justified by the mixed distributional properties of the dataset. The Shapiro-Wilk test indicated that several elements followed distributions close to normality, validating the use of Pearson's coefficient, which assumes linearity and normality. For elements deviating from normality, Spearman's rank correlation was more appropriate, as it is based on ranks, does not require distributional assumptions and is robust to outliers and monotonic but nonlinear relationships. The combined use of both measures thus enabled a more reliable characterisation of co-occurrence patterns, independent of strict statistical assumptions. Notably, even among normally distributed elements, some associations exhibited nonlinear tendencies.

For 30 paired observations ($df = 28$) and a significance level of $p = 0.05$, the critical value of Pearson's correlation coefficient was $|r| \approx 0.361$ (two-tailed test). This means that only correlations with an absolute value greater than this threshold can be considered statistically significant. The number of statistically significant correlations varied across elements, ranging from only two for barium to as many as thirteen for strontium. Most of the significant correlations were positive. The strongest positive relationships were observed between molybdenum and nickel ($r = 0.79$) and between strontium and lithium ($r = 0.79$). High correlations were also found between chromium and nickel ($r = 0.77$), manganese and strontium ($r = 0.72$), aluminum and strontium ($r = 0.70$), as well as between iron and

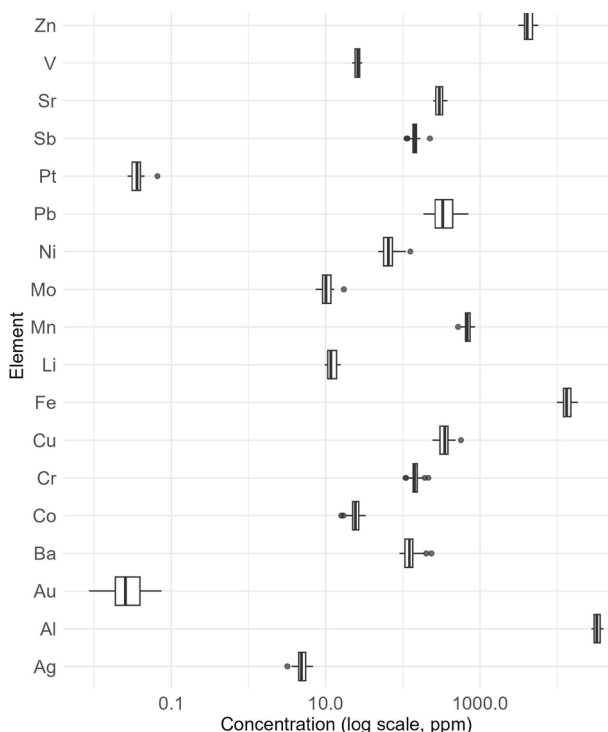


Fig. 2. Distribution of elemental concentration in fly ashes.

manganese ($r = 0.70$), molybdenum ($r = 0.74$) and nickel ($r = 0.71$). Negative correlations were considerably weaker and occurred primarily with barium and gold, with the strongest being between strontium and gold ($r = -0.40$) (Fig. 3A).

Analysis of co-occurrence patterns indicated the formation of two distinct groups. The first cluster linked strontium with lithium, aluminium and manganese. The second was more complex, combining relationships between iron, nickel and molybdenum, together with strong associations among nickel, chromium and molybdenum (Fig. 3B). These clustering patterns highlight both the compositional affinity of certain elements and their potential shared geochemical pathways in fly ash formation.

The lowest number of statistically significant correlations based on Spearman's rank coefficient was observed for gold, with only three significant relationships. In contrast, strontium and zinc exhibited the highest number of significant associations, with 14 correlations each. The strongest nonparametric correlation was a positive association between strontium and lithium ($\rho = 0.78$; Fig. 4A). Other strong positive correlations included iron with nickel ($\rho = 0.76$), iron with manganese ($\rho = 0.73$),

cobalt with copper ($\rho = 0.75$) and lithium with lead ($\rho = 0.70$). Negative correlations were observed mainly for barium and gold, with the strongest being between barium and chromium ($\rho = -0.50$).

Analysis of co-occurrence patterns revealed three main groups of elements. The first cluster comprised strontium and lithium, the second linked iron with both manganese and nickel, while the third was formed by cobalt and copper. These associations underline consistent geochemical affinities within the dataset and are well captured by nonparametric correlation methods (Fig. 4B).

An overall increase in the number of statistically significant correlations was observed when applying Spearman's rank correlation compared with Pearson's linear correlation. For two elements, the number of significant correlations increased by one and three, respectively. In contrast, for three elements (gold, manganese and vanadium), no increase was recorded. In the case of gold, all significant associations were negative and consistently identified with lead, strontium and zinc using both correlation methods. For manganese and vanadium, positive associations were observed with the same elements under both Pearson and Spearman

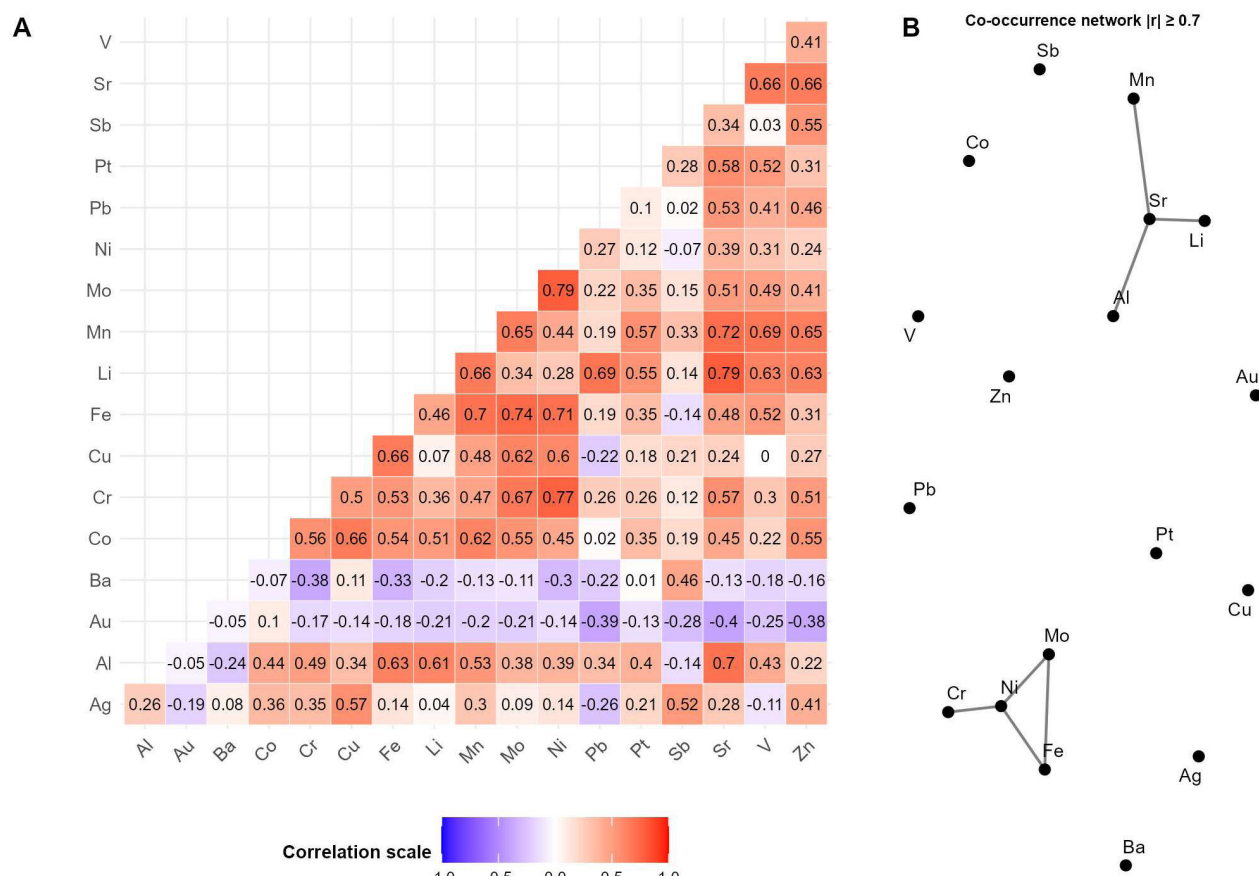


Fig. 3. Pearson correlation matrix and co-occurrence plot. **A** – Pearson linear correlation matrix; **B** – Co-occurrence plot.

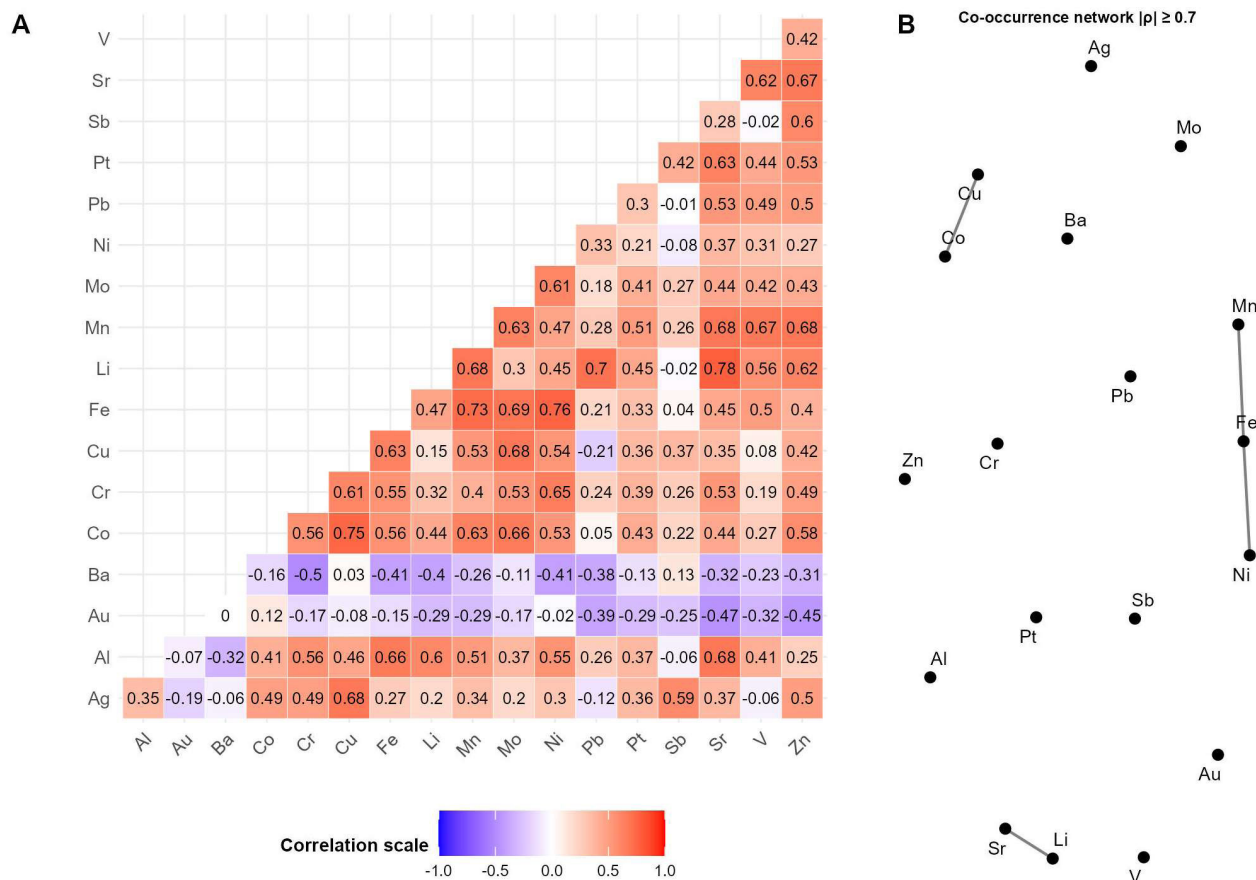


Fig. 4. Spearman correlation matrix and co-occurrence plot. **A** - Spearman rank correlation matrix; **B** - Co-occurrence plot.

approaches. For most elements, however, the number of significant correlations increased by one or two when using Spearman's coefficient, while for silver, barium and copper, the increase was three, and for platinum, as many as six additional significant correlations were identified (Figs. 3A, 4A).

When comparing correlation strengths, differences were generally minor and rarely exceeded 0.05. The largest positive difference in favour of Pearson's correlation was 0.33, observed for the pair antimony-barium. Pearson's coefficient tended to yield stronger correlations (>0.1 higher) primarily for associations involving barium. Conversely, the strongest difference in favour of Spearman's rank correlation was 0.22 for the platinum-zinc pair. Higher Spearman coefficients were more frequently noted for silver, antimony, platinum and copper (Figs. 3A, 4A).

Comparison of the co-occurrence plots further highlighted structural differences between the two methods. Specifically, Spearman's correlation revealed an additional distinct grouping of cobalt and copper. Moreover, the two other clusters

identified were more extensive and interconnected under Pearson's linear correlation, suggesting that parametric and nonparametric approaches capture complementary aspects of the co-association structure among elements (Figs. 3B, 4B).

3.3. Hierarchical cluster analysis

To complement the bivariate correlation results, hierarchical cluster analysis (HCA) was performed in order to identify multivariate associations among elements. By testing several distance metrics and linkage methods, this approach allowed for the evaluation of stable clusters and the broader geochemical structure of fly ash composition. Among the tested variants of hierarchical cluster analysis (HCA), the most distinct partitions were obtained for Euclidean distance combined with Ward, complete and average linkage; for Manhattan distance combined with complete and average linkage; and for 1 - Pearson distance combined with complete linkage. The results of the agglomerative coefficient

(AC) and cophenetic correlation coefficient (CCC) are presented in Table 2, while the corresponding dendrograms are shown in Figure 5.

The quality assessment of the hierarchical clustering demonstrated that the values of the agglomerative coefficient varied depending on the chosen distance metric and linkage method (Table 2). The highest cluster cohesion was observed for the 1 – Pearson + Complete combination (AC = 0.67), suggesting that this configuration produced relatively well-defined groups. In contrast, the cophenetic correlation coefficient, which reflects the degree to

which the dendrogram preserves the original pairwise distances, reached its highest values for Manhattan + Average (CCC = 0.85) and Euclidean + Average (CCC = 0.83). These findings indicate that average linkage approaches most accurately reproduce the data structure, whereas Pearson-based distance provides clearer separation between clusters.

Inspection of the dendrograms reveals consistent clustering patterns across different methods (Fig. 5). Gold and barium formed a distinct cluster in most dendrograms, except for dendrogram C, where they were grouped differently, but in all

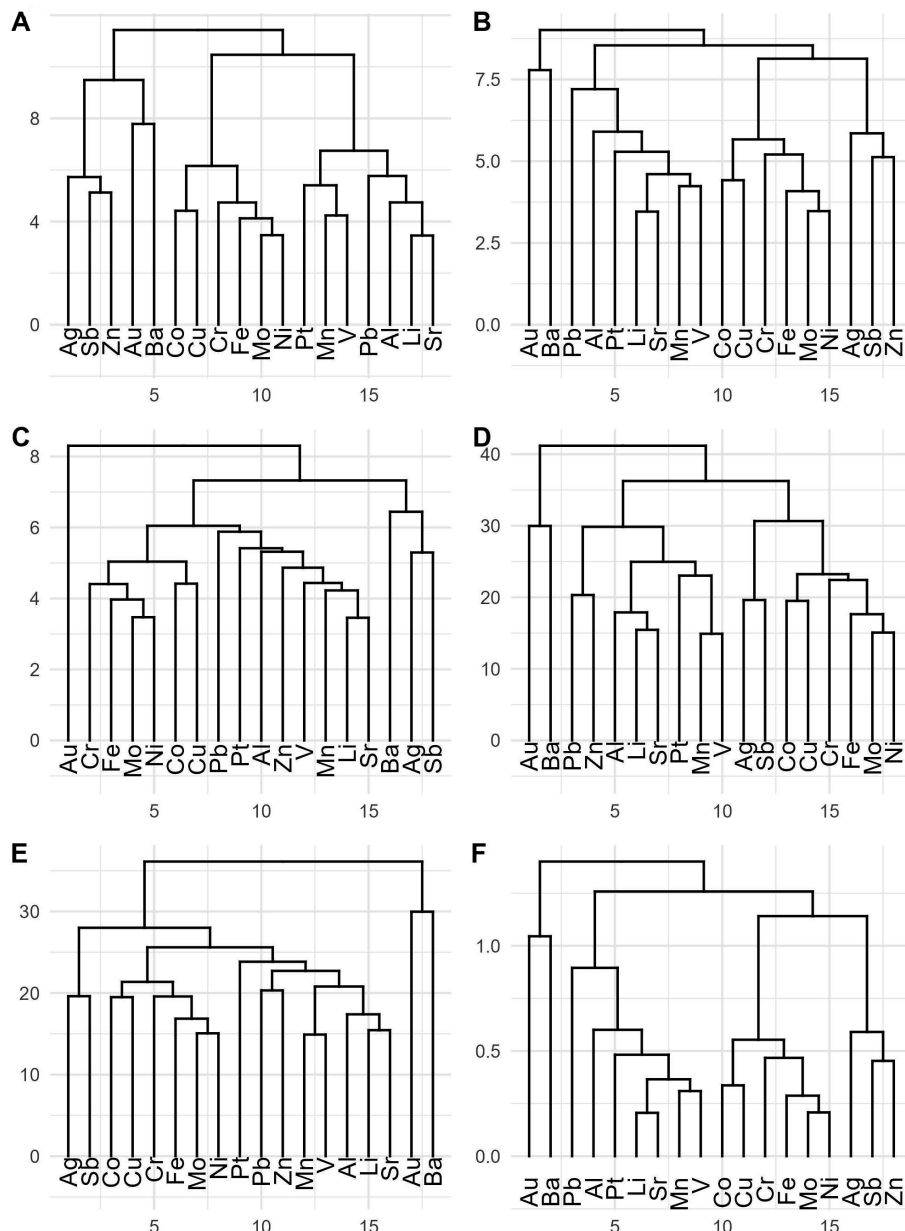


Fig. 5. Hierarchical cluster analysis comparison. **A** – Euclidean distance + Ward.D2 linkage; **B** – Euclidean distance + Complete linkage; **C** – Euclidean distance + Average linkage; **D** – Manhattan distance + Complete linkage; **E** – Manhattan distance + Average linkage; **F** – 1 – Pearson correlation + Complete linkage.

Table 2. HCA agglomerative coefficient and coefficient correlation.

Variant	Agglomerative coefficient	Coefficient correlation
Euclidean + Ward.D2	0.57	0.63
Euclidean + Complete	0.44	0.69
Euclidean + Average	0.42	0.83
Manhattan + Complete	0.53	0.74
Manhattan + Average	0.47	0.85
1-Pearson + Complete	0.67	0.67

cases this cluster exhibited relatively high linkage distances to the remaining groups. Zinc, silver and antimony were frequently clustered together (variants A, B, and F in Figure 5), while in other dendograms silver was consistently paired with antimony. Similarly, chromium, iron, molybdenum and nickel consistently grouped together across all dendograms, often forming a larger cluster when combined with cobalt and copper. Lithium and strontium were also consistently paired, although in larger cluster configurations this group was more mobile and could merge either with lead and aluminium, or with manganese and vanadium. These recurring patterns highlight both the stability and the variability of elemental associations depending on the clustering method applied (Fig. 5).

4. Discussion

The results obtained indicate that fly ash from municipal solid waste incineration (MSWI) facilities is characterised by a highly heterogeneous chemical composition. Statistical analysis shows that most elements occur in a wide range from several tens to several thousand ppm. However, some elements appear in concentrations significantly higher than typical geochemical background levels of the Earth's crust. Particularly notable is the enrichment in zinc (mean 4255 ppm), lead (369 ppm), antimony (144 ppm) and precious metals such as silver (4.96 ppm), gold (0.031 ppm) and platinum (0.036 ppm). For comparison, the average crustal abundances are: zinc – 67 ppm, lead – 17 ppm, antimony – 0.2 ppm, silver – 0.07 ppm, gold – 0.0015 ppm, platinum – 0.0005 ppm (Rudnick & Gao, 2003). Such enrichment clearly suggests that fly ash can be regarded as a potential anthropogenically generated secondary deposit.

At the same time, it is worth noting that for common lithophile elements such as iron (13,640 ppm *vs* 50,000 ppm in the crust), aluminum (33,263 ppm *vs* 82,000 ppm), manganese (688 ppm *vs* 600 ppm, compared to $>300,000$ ppm in Mn ores) and strontium

(301 ppm *vs* 320 ppm in the crust and 439,000 ppm in celestine deposits), fly ash represents a relatively depleted material. Despite their economic importance, these elements cannot be considered viable recovery targets from fly ash due to their insufficient concentrations.

A key issue in the characterisation of fly ash is its heterogeneity. One important finding is the very wide range between maximum and minimum values. For gold, the maximum concentration was nine times higher than the minimum, confirming that precious metals enter the waste stream in an episodic manner – likely due to combustion of small amounts of electronic or jewellery waste. Similar variability was observed for copper and silver, with outliers reaching several thousand ppm. Such anomalies strongly influence the mean values and suggest that recovery of precious metals from fly ash could only be economically feasible in selected material batches enriched in these elements. The heterogeneous composition reflects the variable nature of the waste stream. This confirms previous studies which reported that fly ash differs not only between facilities, but also temporally, e.g. on a weekly or seasonal basis (Buha et al., 2014; Ilyushechkin et al., 2020).

The hierarchical clustering analysis yielded the most distinct partitions for combinations of Euclidean distance with Ward.D2, complete and average linkage; Manhattan distance with complete and average linkage; and 1-Pearson distance with complete linkage. The agglomerative coefficient (AC) and cophenetic correlation (CCC) are summarised in Table 2, with cluster partitions shown in Figure 5. The highest cluster cohesion was obtained for 1-Pearson + Complete (AC = 0.67), whereas the best preservation of data structure in the dendrogram was achieved using average-linkage methods (Manhattan + Average, CCC = 0.85; Euclidean + Average, CCC = 0.83). These results indicate that average-linkage clustering more faithfully represents data structure, while correlation-based distance yields sharper cluster separation.

Cluster analysis further revealed distinct groupings of elements. A stable cluster was formed by Cr-Fe-Mo-Ni, which can be interpreted as reflecting the presence of steel and alloy fractions in MSWI residues. The association Sr-Li-Al-Mn suggests sources linked to ceramics, glass, and building materials. Finally, the Cu-Co cluster points to potential contributions from electronic waste and batteries. Previous studies have emphasised that such groupings are critical for recovery planning, as they enable the design of processes targeting simultaneous extraction of multiple (Fabricius et al., 2020; Funari et al., 2023).

Comparison of fly ash concentrations with ore deposits shows that only a few elements approach economically exploitable thresholds. Zinc reaches over 5700 ppm, overlapping the range typical for Zn-Pb ores (5000–10,000 ppm). Silver reaches values comparable with polymetallic ores (50–300 ppm), while copper in some samples exceeded 4000 ppm, corresponding to the lower boundary of porphyry copper deposits. However, other metals such as antimony, gold, lead and platinum remain far below exploitable ore levels, despite being strongly enriched relative to crustal averages (Singer et al., 2008).

In the context of global mining trends, these findings become particularly significant. Ore grades of major commodities such as copper and nickel have systematically declined over the last decades (Mudd et al., 2017). Thus, even the moderate concentrations of metals in fly ash may acquire increasing economic importance, particularly under the growing pressure to implement circular economy strategies. However, the presence of mobile heavy metals in fly ash poses environmental risks. Elements such as antimony, lead and zinc exhibit high leaching potential under variable pH conditions, as demonstrated by earlier studies on metal mobility in incineration residues (Haberl & Schuster, 2019). Therefore, any recovery strategy must be coupled with stabilisation technologies to minimise environmental impact.

At the same time, several well-established technologies may be adapted for fly ash valorisation, including hydrometallurgical processes (acid leaching, solvent extraction), bioleaching and thermal separation processes allowing volatilisation and condensation of Zn or Pb as salts (Tang & Steenari, 2015; Lane et al., 2020). In some countries, such as Switzerland, industrial-scale facilities already recover Zn and Cu from fly ash. This demonstrates the practical feasibility of such approaches (Schlumberger & Bühler, 2012).

In the framework of urban mining, fly ash should be regarded as a secondary resource with considerable potential but limited strategic significance. The greatest opportunities are associated with zinc and silver recovery, with copper playing a secondary role. Precious metals, although highly enriched relative to background, occur at absolute concentrations that are too low for straightforward economic recovery. Nevertheless, given the rising demand for critical raw materials, development of urban mining technologies should increasingly incorporate this waste stream as a complementary resource alongside primary ores (İşildar et al., 2018; Bakalár et al., 2021).

5. Conclusions

The present study demonstrates that MSWI (municipal solid waste incineration) fly ash represents a material with a complex and heterogeneous chemical composition, containing both abundant lithophile elements and enriched critical and strategic metals. Fly ash is significantly enriched in antimony, gold, lead, silver, platinum and zinc, relative to crustal averages, which clearly supports its consideration as an anthropogenically generated secondary deposit. However, comparison with ore-grade thresholds shows that only zinc, and sporadically silver and copper, approach exploitable levels. This means that fly ash cannot be a substitute for primary deposits, but rather should be considered a complementary resource.

The significance of fly ash within the urban mining framework lies in its contribution to resource diversification and the reduction of pressure on primary ore extraction, aligning with circular economy principles and EU raw materials policy. Importantly, recovery processes must always be coupled with stabilisation technologies due to the presence of mobile and toxic metals such as lead and antimony. A combination of hydrometallurgical, bioleaching and thermal separation methods could enable recovery, although the economic viability depends on metal concentrations in specific material fractions and further technological development.

Looking forward, the role of fly ash in resource supply is expected to grow over the coming decades. This trend is driven by two main factors: (i) the ongoing depletion and declining grades of primary ores, and (ii) the increasing demand for critical metals related to energy transition and digitalisation. Under these conditions, even medium-grade resources such as fly ash may become strategically relevant, especially as supplementary sources of copper, silver and zinc. With the implementation of innovative recovery technologies and greater integration of urban mining concepts into raw materials policy, fly ash may evolve into a permanent component of Europe's resource mix, reducing import dependency and supporting the development of a sustainable circular economy.

Acknowledgements

This research project was partly supported by the AGH University of Krakow, Faculty of Geology, Geophysics and Environmental Protection, as a part of a statutory project. Moreover, it was co-financed by the programme 'Excellence initiative – research university' for the AGH University.

We deeply appreciate comments, suggestions and corrections of two anonymous reviewers.

Authors' contributions

B.B. and M.C.: conceptualization, methodology, writing – original draft preparation, writing – review and editing, investigation, supervision; M.C.: formal analysis, visualization; B.B.: project administration. All authors have read and agreed to the published version of the manuscript.

Conflicts of interest

The authors declare that they have no known competing financial interests or personal relationships that could have appeared to influence the work reported in this paper.

References

Assi A., Bilo F., Zanoletti A., Ponti J., Valsesia A., La Spina R., Zacco A. & Bontempi E., 2020. Zero-waste approach in municipal solid waste incineration: Reuse of bottom ash to stabilize fly ash. *Journal of Cleaner Production* 245, 118779.

Bakalár T., Pavolová H., Hajduová Z., Lacko R. & Kyšeľa K., 2021. Metal recovery from municipal solid waste incineration fly ash as a tool of circular economy. *Journal of Cleaner Production* 302, 126977.

British Geological Survey, 2025. Minerals UK. website: <https://Www.Bgs.Ac.Uk/Mineralsuk//> (accessed on 20.08.2025).

Buha J., Mueller N., Nowack B., Ulrich A., Losert S. & Wang J., 2014. Physical and chemical characterization of fly ashes from Swiss waste incineration plants and determination of the ash fraction in the nanometer range. *Environmental Science & Technology* 48, 4765–4773.

Fabricius A.L., Renner M., Voss M., Funk M., Perfoli A., Gehring F., Graf R., Fromm S. & Duester L., 2020. Municipal waste incineration fly ashes: from a multi-element approach to market potential evaluation. *Environmental Sciences Europe* 32, 88.

Funari V., Toller S., Vitale L., Santos R.M. & Gomes H.I., 2023. Urban mining of municipal solid waste incineration (MSWI) residues with emphasis on bioleaching technologies: a critical review. *Environmental Science and Pollution Research* 30, 59128–59150.

Fuoco R., Ceccarini A., Tassone P., Wei Y., Brongo A. & Francesconi S., 2005. Innovative stabilization/solidification processes of fly ash from an incinerator plant of urban solid waste. *Microchemical Journal* 79, 29–35.

Haberl J. & Schuster M., 2019. Solubility of elements in waste incineration fly ash and bottom ash under various leaching conditions studied by a sequential extraction procedure. *Waste Management* 87, 268–278.

Hand D.J., Smyth P. & Mannila H., 2001. *Principles of Data Mining*. MIT Press, website: <https://doi.org/10.1201/b10158> (accessed on 20.08.2025).

Hauke J. & Kossowski T., 2011. Comparison of values of Pearson's and Spearman's correlation coefficients on the same sets of data. *Quaestiones Geographicae* 30, 87–93.

Headrick T.C., 2016. A note on the relationship between the Pearson product-moment and the Spearman rank-based coefficients of correlation. *Open Journal of Statistics* 06(06).

Huang S.C., Chang F.C., Lo S.L., Lee M.Y., Wang C.F. & Lin J.D., 2007. Production of lightweight aggregates from mining residues, heavy metal sludge, and incinerator fly ash. *Journal of Hazardous Materials* 144, 52–58.

Ilyushechkin A., He C. & Hla S.S., 2020. Characteristics of inorganic matter from Australian municipal solid waste processed under combustion and gasification conditions. *Waste Management & Research* 39, 928–936.

İşildar A., Ren E.R., van Hullebusch E.D. & Lens P.N.L., 2018. Electronic waste as a secondary source of critical metals: Management and recovery technologies. *Resources, Conservation and Recycling* 135, 296–312.

Ivan Diaz-Loya E., Allouche E.N., Eklund S., Joshi A.R. & Kupwade-Patil K., 2012. Toxicity mitigation and solidification of municipal solid waste incinerator fly ash using alkaline activated coal ash. *Waste Management* 32, 1521–1527.

Joseph A., Snellings R., Van den Heede P., Matthys S. & De Belie N., 2018. The use of municipal solid waste incineration ash in various building materials: A Belgian point of view. *Materials* 11, 141.

Kabata-Pendias A., 2011. *Trace Elements in Soils and Plants* (4th ed.). CRC Press, website: <https://doi.org/10.1201/b10158> (accessed on 20.08.2025).

Kalmykova Y. & Karlfeldt Fedje K., 2013. Phosphorus recovery from municipal solid waste incineration fly ash. *Waste Management* 33, 1403–1410.

Kanhar A.H., Chen S. & Wang F., 2020. Incineration fly ash and its treatment to possible utilization: A review. *Energies* 13, 6681.

Kara F., 2021. Comparison of tree diameter distributions in managed and unmanaged Kazdağı fir forests. *Silva Balcanica* 22, 31–43.

Kravtsova M.V. & Volkov D.A., 2015. Methodology of research for qualitative composition of municipal solid waste to select an optimal method of recycling. *IOP Conference Series: Materials Science and Engineering* 91, 012075.

Lane D.J., Hartikainen A., Sippula O., Lähde A., Mesceriakovas A., Peräniemi S. & Jokiniemi J., 2020. Thermal separation of zinc and other valuable elements from municipal solid waste incineration fly ash. *Journal of Cleaner Production* 253, 120014.

Lima A.T., Ottosen L.M., Pedersen A.J. & Ribeiro A.B., 2008. Characterization of fly ash from bio and municipal waste. *Biomass and Bioenergy* 32, 277–282.

Mudd G.M., Jowitt S.M. & Werner T.T., 2017. The world's lead-zinc mineral resources: Scarcity, data, issues and opportunities. *Ore Geology Reviews* 80, 1160–1190.

Murtagh F. & Contreras P., 2011. *Methods of hierarchical clustering*. Computing Research Repository – CORR.

Nielsen F., 2016. Hierarchical clustering. [In:] Introduction to HPC with MPI for data science. Springer International Publishing, 195–211.

PN-EN 14899: 2006. Polski Komitet Normalizacyjny, 2006. PN-EN 14899 *Charakteryzowanie odpadów – Pobieranie próbek materiałów – Struktura przygotowania i zastosowania planu pobierania próbek* [Characterization of waste – Sampling of waste materials – Framework for the preparation and application of a sampling plan].

Prasittisopin L., 2024. Power plant waste (fly ash, bottom ash, biomass ash) management for promoting circular economy in sustainable construction: emerging economy context. *Smart and Sustainable Built Environment*, website: <https://doi.org/10.1108/SAS-BE-09-2024-0395> (Accessed on 20.08.2025).

Rosner B., 1983. Percentage Points for a Generalized ESD Many-Outlier Procedure. *Technometrics* 25, 165–172.

Rudnick R.L. & Gao S., 2003. Composition of the continental crust. *Treatise on Geochemistry* 3, 1–64.

Rusănescu C.O. & Rusănescu M., 2023. Application of fly ash obtained from the incineration of municipal solid waste in agriculture. *Applied Sciences* 13, 3246.

Schlumberger S. & Bühler J., 2012. Urban mining: Metal recovery from fly and filter ash in waste to energy plants. *Ash Utilisation 2012 – Ashes in a Sustainable Society*. Stockholm, Sweden.

Shapiro S.S. & Wilk M.B., 1965. An analysis of variance test for normality (complete samples). *Biometrika* 52, 591.

Singer D.A., Berger V.I. & Moring B.C., 2008. *Porphyry copper deposits of the world: Database and grade and tonnage models*. website: <https://Pubs.Usgs.Gov/0f/2008/1155/> (accessed on: 20.08.2025).

Sobianowska-Turek A., 2018. Hydrometallurgical recovery of metals: Ce, La, Co, Fe, Mn, Ni and Zn from the stream of used Ni-MH cells. *Waste Management* 77, 213–219.

Sokal R.R. & Rohlf F.J., 1962. The comparison of dendograms by objective methods. *Taxon* 11, 33–40.

Tang J. & Steenari B.M., 2015. Solvent extraction separation of copper and zinc from MSWI fly ash leachates. *Waste Management* 44, 147–154.

U.S. Geological Survey, 2021. 2021 Minerals Yearbook. website: <https://Pubs.Usgs.Gov> (accessed on 20.08.2025).

U.S. Geological Survey, 2024. *Mineral Commodity Summaries*. website: <https://Pubs.Usgs.Gov/Periodicals/Mcs2024> (accessed on 20.08.2025).

Valero A. & Valero A., 2014. *Thanatia: the destiny of the Earth's mineral resources. A thermodynamic cradle to cradle assessment*. World Scientific, Singapore, 629 pp.

Wang P., Li J., Hu Y. & Cheng H., 2023. Solidification and stabilization of Pb-Zn mine tailing with municipal solid waste incineration fly ash and ground granulated blast-furnace slag for unfired brick fabrication. *Environmental Pollution* 321, 121135.

Wong S., Mah A.X.Y., Nordin A.H., Nyakuma B.B., Ngadi N., Ma, R., Amin N.A.S., Ho W.S. & Lee T.H., 2020. Emerging trends in municipal solid waste incineration ashes research: a bibliometric analysis from 1994 to 2018. *Environmental Science and Pollution Research* 27, 7757–7784.

Yakubu Y., Zhou J., Ping D., Shu Z. & Chen Y., 2018. Effects of pH dynamics on solidification/stabilization of municipal solid waste incineration fly ash. *Journal of Environmental Management* 207, 243–248.

Zierold K.M. & Odoh C., 2020. A review on fly ash from coal-fired power plants: chemical composition, regulations, and health evidence. *Reviews on Environmental Health* 35, 401–418.

Manuscript submitted: 30 August 2025

Revision accepted: 23 September 2025